Pertanika J. Soc. Sci. & Hum. 21 (4): 1491 - 1515 (2013)

PERTANIKA JOURNALS

SOCIAL SCIENCES & HUMANITIES

Journal homepage: http://www.pertanika.upm.edu.my/

# Thermal Comfort Investigation in Traditional and Modern Urban Canyons in Bandar Abbas, Iran

**Masoud Dalman[1], Elias Salleh[1], Abdul Razak Sapian[2] and Omidreza Saadatian[3]***

*[1]Faculty of Design and Architecture, Universiti Putra Malaysia, 43400 Serdang, Selangor, Malaysia*
*[2]Department of Architecture, Kulliyyah of Architecture and Environmental Design, International Islamic University of Malaysia, P.O. Box 10, 50728 Kuala Lumpur, Malaysia*
*[3]Solar Energy Research Institute, Universiti Kebangsaan Malaysia, Perpustakaan Tun Sri Lanang, Universiti Kebangsaan Malaysia, 43600 Bangi, Selangor, Malaysia*

## ABSTRACT

Urban design plays an important role in a city's daily life. Therefore, accessibility to thermal comfort spaces for citizens engaged in urban outdoor activities could be one of the main goals of urban designers. Urban forms and canyons have important roles in microclimate and thermal comfort situation in outdoor spaces. The hot humid climate of Bandar Abbas, especially in long summers, causes thermal stress for urban activities. In this study, two different urban fabrics were investigated using thermal comfort and Computational Fluid Dynamics (CFD) methods. Eight provisional measuring points in the selected prevailing canyons were used to obtain the data. The results correlated with the effects of the urban canyon orientation to variation of the microclimate factors, and consequently, the thermal comfort situation in the hottest period of the year. In addition, the results also indicated that the traditional urban fabric is more thermally comfortable than the new residential urban fabric. According to field measurements, thermal comfort calculation and wind simulations, the canyons with the north-south direction present a better orientation for air circulation benefiting from the sea breezes as compared to the other canyon orientations. Hence, this study provides insights for urban designers and policy makers residing in the hot and humid climate in the Middle East.

ARTICLE INFO

*Article history:*
Received: 27 September 2011
Accepted: 13 February 2012

*Keywords:* Microclimate, hot-humid, urban canyon, thermal comfort, Computational Fluid Dynamics

*E-mail addresses*:
masoud_dalman@yahoo.com (Masoud Dalman),
elsall06@gmail.com (Elias Salleh),
razak@gmail.com (Abdul Razak Sapian),
omid.saadatian@gmail.com (Omidreza Saadatian)
* Corresponding author

## INTRODUCTION

Bandar Abbas is a big port in southern Iran, which has experienced a rapid growth of urban area, population, shipping, industrial,

ISSN: 0128-7702 

and commercial services since 1980; the year that marked the start of the Iran-Iraq war. This rapid growth has caused drastic changes in urban microclimate that has adverse impacts on human thermal comfort in the hot period of summers. There are very few studies on the climate response in urban planning and design during hot and humid periods, particularly in the southern part of Iran and the Persian Gulf regions (Thapar, 2008). Therefore, the necessity of urban climate studies in the mentioned regions could be a big concern of the urban planners and designers.

Among the climatic regions of Iran, there lies the hot and humid region with long summers and short days in short moderate winters along the narrow coastal strip of the Persian Gulf and the Oman Sea. The length of this hot and humid region is almost 2000 kilometres (Shouhian *et al.,* 2005). In this region, relative humidity and temperature are high during critical summer months. Besides, Heidari and Sharples (2002) argued that the diurnal temperature difference is rather low in this part of Iran compared to those for the inland regions of the country, as shown in Fig.1. This city's climate is a specific one because of its high humidity, in which cooling of this kind of climate is dependent upon evaporation and moisture entransy (Chen *et al.,* 2011). According to the weather data of Bandar Abbas meteorological station, the summer months experience steady and stable weather conditions. In this period, no gusty winds, rainy days and storms have been recorded. However, the Indian Ocean monsoon rain covers the mountainous areas from June until September.

The city of Bandar Abbas is located on a flat ground, i.e. at 10 m above the mean sea level at the latitude of 27˚11' N and the longitude of 56˚22'E. Every year, Bandar Abbas experiences eight months of harsh condition of heat from April to November (Heidarin & Sharples, 2002).

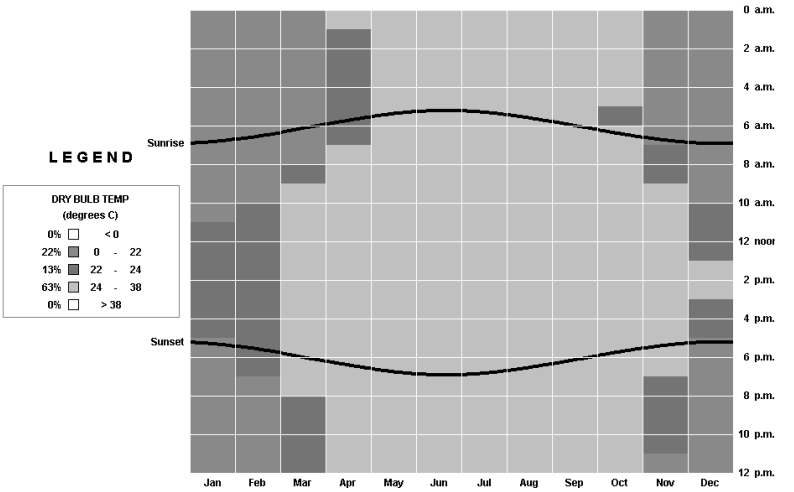


Fig.1: Monthly variations of air temperature in Bandar Abbas (adapted from IMO, 2010)

This study has two main objectives. The first objective was to find out the relation between thermal comfort situation and microclimatic characteristics of urban canyons within the different fabrics (Fig.2) in the hottest period of summers, particularly in July, which is the hottest month of the year. Meanwhile, the second objective was to determine the role of the urban canyon orientation and dimension on wind circulation.

## LITERATURE AND THEORIES

Existing literature supports the influence of urban design on cities' thermal comfort conditions. For instance, Ali-Toudert and Mayer (2007) ascertained the impacts of vertical profile and orientation of the urban canyon on human thermal sensation at the street level, while Nunez and Oke (1977) proposed the use of urban canyons with simplified rectangular vertical profiles of infinite lengths as the basic structural units for a typical urban open space in urban climatology. Conversely, Johansson (2006) ascertained the impacts of various features of physical structure of cities on urban climate by focusing on the effects of the average height of buildings on wind speed and direction. Likewise, Johansson and Emmanuel (2006) believe that the urban climate and outdoor thermal comfort at street level are significantly influenced by the urban form. Moreover, they claimed that the relationship between urban design and outdoor thermal comfort in hot and humid climates should be understood for developing appropriate climate-oriented urban design guidelines. Johansson and Emmanuel (2006) further concluded that the urban thermal comfort is significantly influenced by the affecting factors, which include the height-to-width (H/W) ratio of the urban canyons, street orientations,

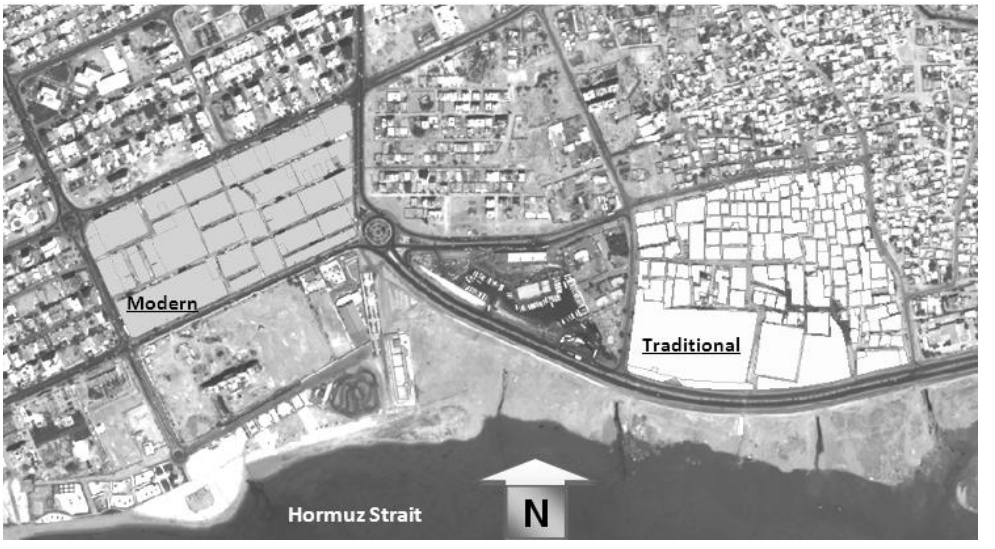


Fig.2: A satellite image of the selected fabrics (Source: Google Earth, 2010)

ground covers, and distance from the shore. On the same account, Givoni (1998) believe that the urban climate mostly depends on the arrangement of buildings with different heights in the cities. He also claimed that the urban climate can be controlled by the urban planning and design since the structure of the city can be controlled by the urban features. Furthermore, he also ascertained that the buildings in urban area usually have thermal comfort problems due to their poor planning and climate consideration. Thus, based on the latter discussion, the most important factors in urban thermal comfort are the influence of wind gustiness and mean instantaneous wind speed. Combining these facts, the research concludes that wind has the greatest influence on urban thermal comfort. Material and methods

## MATERIALS AND METHODS

This study adopted the empirical research method. More precisely, field measurements were employed by considering climatic factors; namely, wind speed, relative humidity and air temperature, for the investigation of thermal comfort and microclimate situation. The Computational Fluid Dynamics (CFD) simulations of wind speed were also conducted as the predictive models. The field measurements were taken for ten days, from 1st to 10th July (2010), for air temperature and relative humidity at eight different locations (i.e. four points in each fabric) in a walking distance from each point of the selected fabric (Fig.3). However, wind speed was measured from 1st to 5th July. This period could be taken as a reliable indicator for the hottest days of the year in July, with a stable weather situation and a series of days with a similar condition according to the weather data of Bandar Abbas (IMO, 2010). Apparently, a rather similar data collection period from 9th to 15th July was chosen by Thapar (2008) in a comparative study carried out in Dubai.

### *Context of measurements*

A comparative investigation was conducted to discover the impacts of urban form and layout on the variation of the microclimatic factors and thermal comfort situation in

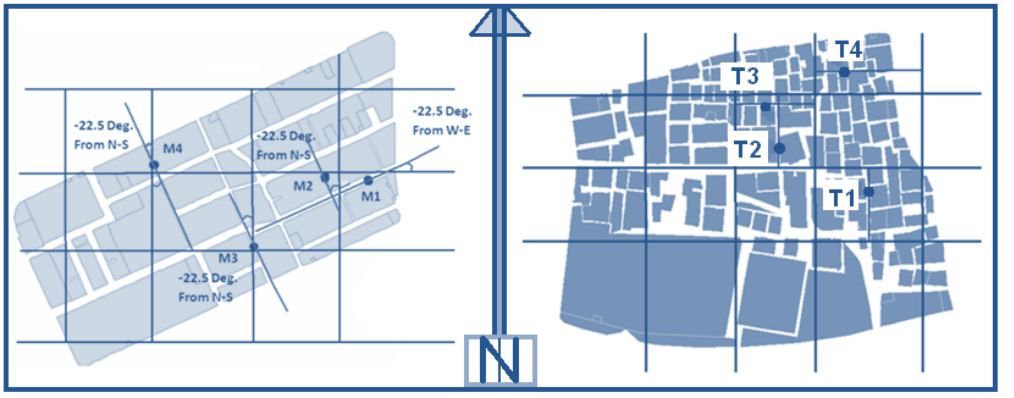


Fig.3: The direction of prevailing canyons in each fabric

two urban areas. These two areas are the typologies of the southeast of Bandar Abbas, which are considered as suitable samples for both the traditional and modern fabrics adjacent to each other. Therefore, the two representative areas were selected as the contexts of measurements and thermal comfort investigations. Both selected areas are located near the sea shore. The two selected different fabrics are separated by an N-S street in southeast of Bandar Abbas. The selected areas could be good representatives for all the urban areas of Bandar Abbas as they comprise both traditional (TR) and modern (MD) fabrics that are next to each other. Furthermore, they also have similar attributes in terms of microclimate, location, distance to the sea shore, and influence of sea breezes. Besides, both the traditional and modern parts of the selected areas are covered by houses with the same typology comprising courtyards and single-story buildings. The traditional fabric is called Nakhl-e-Nakhoda (Captain Palm), whereas the new residential development is called Golshahr-e-Jonoobi (South Golshahr). Table 1 and Table 2 summarize the specifications of the two different selected fabrics.

As shown in Table 1 and Table 2, the traditional fabric has a larger area than the modern fabric. By using the ArcMap software, the rate of the pathway coverage in the modern fabric is 20%, whilst in the traditional fabric, the pathway coverage is 26% (Esri, 2008). Hence, the higher pathway coverage could expedite air circulation in the traditional area with the S-N canyon orientation rather than the modern fabric with the WSW-ENE prevailing canyon orientation. According to the prevailing wind direction of Bandar Abbas (from southward), the traditional canyons could be ventilated by the prevailing wind through the whole area.

A satellite image of the two selected fabrics (Fig.2) demonstrates the prevailing canyon patterns such as orientation, dimension and open spaces, based on the

TABLE 1
Specifications of the selected fabrics

| Fabric | Area(Hectare) | Perimeter(Meter) | Pathways coverage ratio (%) | Buildings coverage ratio (%) |
|---|---|---|---|---|
| Traditional | 19.3 | 3254.3 | 26% | 74% |
| Modern | 12.8 | 1531.4 | 20% | 80% |

TABLE 2
Inventory of the selected canyons

| Site | Type | H/W Ratio | Prevailing Orientation | Vehicle Traffic | Ground Cover | Distance from Sea(m) | Distance between fabrics (m) | Fabric specification |
|---|---|---|---|---|---|---|---|---|
| South Golshahr | Residential | 0.5 | WSW-ENE | Medium | Asphalted | 438 | 790 | New Development |
| Nakhl-e-Nakhoda | Residential | 1 | N-S | Low | Sandy | 380 | | Traditional |

information from the master plan of Bandar Abbas (Sharmand, 2008). The distance between the two fabrics and Bandar Abbas weather station is around 3km. In terms of the canyon deviation from the main geographical directions, Fig.3 illustrates that in the modern fabric, the deviation of the N-S canyons is about -22.5 degree from the north, whereas for the E-W canyons, it is about -22.5 degree from the east. Consequently, while the exact direction of M1 and M2 is WSW-ENE, it is SSE-NNW for M3 and M4. In the traditional fabric, the canyon directions are N-S for T1 and T2, and W-E for T3 and T4.

**Modern Fabric**

The south area of Golshahr (SG) consists of courtyard houses constructed by private owners during the 1980s. However, the main street sides were reconstructed after the year 2000 with medium and high-rise commercial and residential buildings. In the recent 10 years, the bare interior lands have also been under construction of medium rise buildings. However, to maintain the consistency in a comparative analysis, the selected canyons in SG mainly comprise single-story courtyard houses, which are similar to the houses in the traditional fabric. The specifications of the fabric canyons are presented in Table 3.

As illustrated in Fig.4, although the prevailing canyons in this fabric are extended along the WSW-ENE orientation, the subsidiary access alleys have the SSE-NNW orientation. The width of the prevailing canyons varies from 6m to 12m, whereas the width of the subsidiary canyons varies between 1.5m to 3m (Sharmand, 2008).

There were four selected canyons in the modern fabric, namely, M1, M2, M3, and M4. The descriptions of these canyons are as follows:

M1: This is a predominant type of canyon in the modern fabric, in which 80% of the fabric canyons have the same layout and dimension with the WSW-ENE orientation. The H/W ratio of this canyon is 0.5, whereas the street width is 7.50m according to the master plan of Bandar Abbas.

M2 and M4: This kind of canyon mainly comprises secondary alleys with smaller dimensions than those for the M1 category. The main criterion in selecting these canyons was that these canyons resemble the traditional fabric

TABLE 3
Specifications of the modern fabric canyons

| Canyon | Width (m) | Wall Height (m) | | Canyon Orientation | H/W Ratio |
|---|---|---|---|---|---|
| M1 | 7.5 | S=3.50 | N=4.00 | WSW-ENE | 0.5 |
| M2 | 1.85 | E=3.15 | W=3.00 | SSE-NNW | 1.7 |
| M3 | 4.85 | E=4.40 | W=7.50 | SSE-NNW | 1.2 |
| M4 | 3.15 | E=3.50 | W=3.40 | SSE-NNW | 1.1 |

(E=Eastern, W=Western, N=Northern, S=Southern)

canyons. This includes the width, wall height and H/W ratio so that a comparison between them in the same circumstances and weather conditions could be meaningful. As presented in Table 3, the canyon widths and building heights for M2 and M4 measure 1.85 and 3.15m (width) and 3.40 and 3.50m (height), respectively.

M3: As presented in Fig.3, this canyon is located in the southern part of the modern fabric, which is closer to the sea shore with almost more unique dimensions than the other canyons in this area. The width of this canyon is 4.85m, while the heights measure 7.5m and 4.40m.

**Traditional Fabric (Nakhl-e-Nakhoda)**

The history of this quarter could be traced back to a separated fishing village located 10 km away from the historical city of Bandar Abbas over two hundred years ago. With the rapid development of urban areas, especially over the recent 30 years, this part has been attached to the urban area. Yet, it still preserves its traditional form. However, some illegal houses and sprawl fabrics have been formed in the eastern and northern parts of this district since 1991. This fabric is basically located along the coastline, and the selected canyons belong to the traditional part of this area with narrow and spiral lanes and sandy pathways, develop towards the coastline and have a seaward orientation (Shohouhian *et al.,* 2005). The canyon setting in this fabric is designed to allow air circulation through the urban canyons. Furthermore, it is also designed to use tall buildings and vegetation for reducing the heat by providing more effective shades (Najafabdi *et al.*, 2006). Consequently, the general orientation of the urban setting in this region follows the directions of coastline and wind, whereby the streets and paths are arranged as to catch the pleasant winds coming from the sea (Ghobadian,

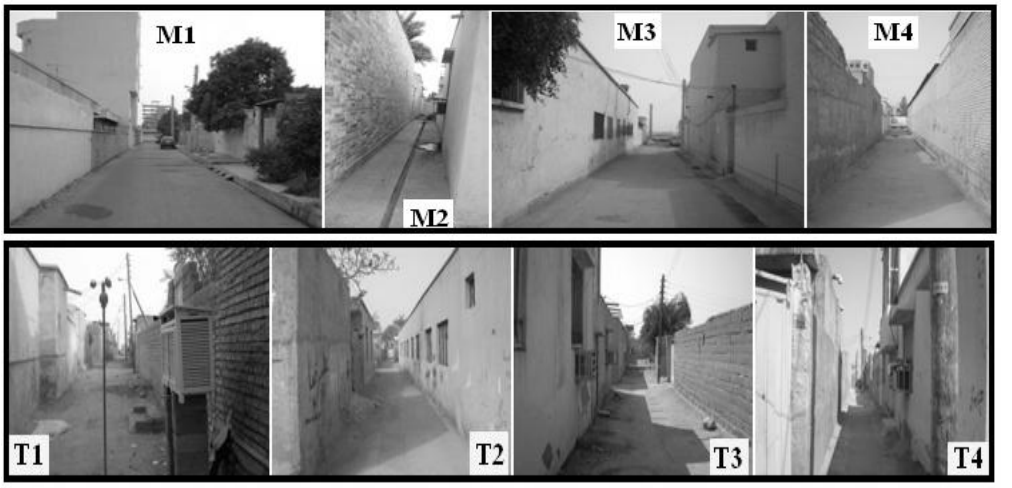


Fig.4: The selected prevailing canyons of the traditional and modern fabrics

1998). The prevailing canyon orientation in this fabric is S-N. Further explanations on the features of this fabric are presented in Table 4.

Majority of the houses (90%) in this area consist of terraced units with courtyards, while almost 10% are detached single units (Alaedini *et al.*, 2008). The detached single units with yards serve dual purposes of importance; firstly, they allow the flow of air for reducing humidity, and secondly, they reduce damages from earthquakes, which is an important point since the region is an earthquake prone area. The walls and roofs of these units are constructed from solid and long lasting materials. Nevertheless, it should be noted that these structures do not meet the minimum building code standards.

As shown in Fig.3, there were four selected canyons in this fabric; namely, T1, T2, T3, and T4. T1 and T2 are two common canyons in the traditional fabric. From the figure, it shows that 90% of the canyon region has the S-N orientation, deep alleys and sandy pavement. The average width of such canyons is 2-3m, while the average building height is 3.6m, with the H/W ratio of 0.95 to 1.4. As for T3 and T4, despite the predominant S-N orientation of canyons in the traditional fabric, the two are the type of canyons that are formed along the W-E orientation. The main reason for selecting these canyons was their similarity to the modern fabric canyons so that a comparison between them in the same weather condition could be meaningful. The H/W ratios of these canyons are 0.95 and 1.4, whereas the widths are 4.00m and 2.35m, respectively. In spite of the similar orientations, the differences in the width and H/W have caused the variation in shading effect, air temperature and wind speed.

## MICROCLIMATE OBSERVATION AND DATA MEASUREMENT

Field measurements using the weather instruments were carried out in this study. Some meteorological instruments such as thermometer, anemometer and humidity sensor were continuously used to investigate the variation of microclimate factors during the data collection period. Thus, comparability is the key criterion in selecting the sites for the measurements conducted in this study area in July 2010.

In this study, air movement was measured using the "Muller 91g" counter anemometer for measuring wind run usable for velocities from 0.6 to 60 m/s (Muller, 2005). This kind of anemometer consists

TABLE 4
Specifications of the selected canyons in the traditional fabric

| Canyon | Width (m) | Wall Height (m) | | Canyon Orientation | H/W Ratio |
|---|---|---|---|---|---|
| T1 | 3.80 | E=3.65 | W=3.60 | S-N | 0.95 |
| T2 | 3.20 | E=3.70 | W=3.60 | S-N | 1.1 |
| T3 | 4.00 | N=2.50 | S=3.80 | E-W | 0.95 |
| T4 | 2.35 | N=3.30 | S=3.20 | E-W | 1.4 |

(E=Eastern, W=Western, N=Northern, S=Southern)

of a three-armed cup wheel with conical cups and a seven-digit reel counter that indicate wind movement in km with the accuracy of reading 10m, 250mm in height and 3.25kg in weight. The wind speed data were registered in a one-hour interval of 24 hours from 1st to 5th July 2010 at a two-meter height in the middle of each canyon. Meanwhile, the air temperature and relative humidity were recorded in a 15-minute interval of 24 hourly from 1st to10th July 2010 using the Hobo data logger (model: H08-004-02). The findings revealed a temperature measurement range of -20°C to 70°C (-4°F to 158°F) and a humidity range of 0 to 95% of RH non-condensing, non-fogging (Onset, 2004). This range is a good match to the expected summer time temperature and humidity range of 30 to 45°C and 40 to 95% in Bandar Abbas. The data from the meteorological station at Bandar Abbas International Airport (BAIA), with the height of 10m from the sea level and located 3.5km away from the modern fabric and 2.8km from the traditional fabric, were considered as the reference data in the data assessments.

Some similar studies also used the Hobo sensors for studying hot and humid climates. For instance, Sullivan and Collins (2009) studied the evaluation of an urban heat island in Tampa, Florida, while Yu and Hien (2006) investigated the thermal effects of city greens on the surroundings under the tropical climate in Singapore. In addition, Balázs *et al.* (2009) studied the effects of microclimate in a high-rise residential in Singapore. Likewise, Krüger *et al.* (2010) evaluated the impacts of street geometry on ambient temperatures and daytime pedestrian comfort levels in Curitiba, Brazil. They emphasized the effectiveness and accuracy of the Hobo sensors in measuring outdoor air temperature and relative humidity.

*Measurement Error Analysis*

In this study, the recorded data had possible errors in measuring the accuracy rate of the instruments. The data of this research were collected via three kinds of observations; namely, systematic, direct, and software calculations. The direct observation included field measurements comprising canyon dimensions, which were measured by utilizing the measurement devices and ArcMap software; wind speed, which was measured via the anemometers; as well as air temperature and relative humidity, which were measured by employing the Hobo data loggers. The calculations of thermal comfort indices and air flow predictions were conducted by using the RayMan and MicroFlo (IESve) programmes.

According to the true space theory, the true score of a research work is calculated as a summation of truth and measurement errors. Equation var*(X)* below is the *observation score*, where var (*T*) is the *trough ability*, and var ($E_X$) is the *random error* (Creswell, 1994):

$$var(X) = var\ (T) + var\ (E_X)$$

Therefore, measurement errors contain random errors and systematic errors, which are related to the following equation:

$$X= T+Er+Es$$

Therefore, minimizing the random error and systematic error was considered in this research. In order to get more accurate results for controlling the random error in the systematic observation phase of this research, firstly, all the measurement instruments were tested in the pilot tests with the reference station equipment, simultaneously, then the data were measured, and finally, the findings were verified with the reference station data and double-checked thoroughly. Consequently, the triangulation of the findings of the three phases neutralized the random error (Creswell, 1994). Lastly, potential errors from the Rayman programme and simulation software (MicroFlo) were minimized by using accurate microclimate and physical data from the field measurements. The accuracy rates of instruments (i.e. Hobo data logger and Muller anemometer) are as follows:

Hobo data logger: time accuracy = ±1 Minute per week at 20°C, humidity sensor ±5% and air temperature sensor, ±0.7°C at + 21.1 °C.

Muller anemometer: ±10 m in each recorded km/h

These accuracy rates of the recording equipment are acceptable, and the random errors were found to be less than 5%, which meant the measurements exhibited a good accuracy of around 95%.

*Microclimate observation*

The climate data of local environment were the main parts of the microclimate analysis. According to the recorded data of the selected canyons, the hourly data of wind speed (1-5 July), air temperature and relative humidity (1-10 July) in the hottest period of the year were measured. The July period was selected for the evaluation of thermal comfort for the maximum thermal stress in the study area.

**Relative Humidity and Air Temperature**

The length of a sultry period in the study area is more than six months (see Fig.5). The results of relative humidity of Bandar Abbas weather station from 1959-2005 (46 years) showed that the maximum annual RH percentage was 100%, with an average of the maximum annual of RH% during this period of 99.4% and an average of 65.3% in the 46-year data. Thus, in approximately 8 to 10% of the year, the sultry and RH rates were over 90%. Evidently, the highest occurrence rate of RH% in the study area was reported to be around 60% to 70 % (Esfandiarnejad, 2010).

**Air movement**

One of the important wind phenomena in the coastal regions is the land and sea breezes. These winds are developed by the differential heating and cooling over the land and sea (Hamdan *et al.,* 2007). The sea

breeze begins at about 9 am, blows with the greatest force in the early afternoon around 2-3 pm, and becomes lighter at sunset. During the nights, the wind speed is less than 0.1m/s. Based on the geographical condition of Bandar Abbas and the Persian Gulf influences, the prevailing wind of a year is southward and the average wind speed is around 6 m/s. Fig.6 shows the monthly variations of wind speed in Bandar Abbas (IMO, 2010).

As the urban areas are often highly affected by their form and region climate (Toudert & Mayer, 2007), their

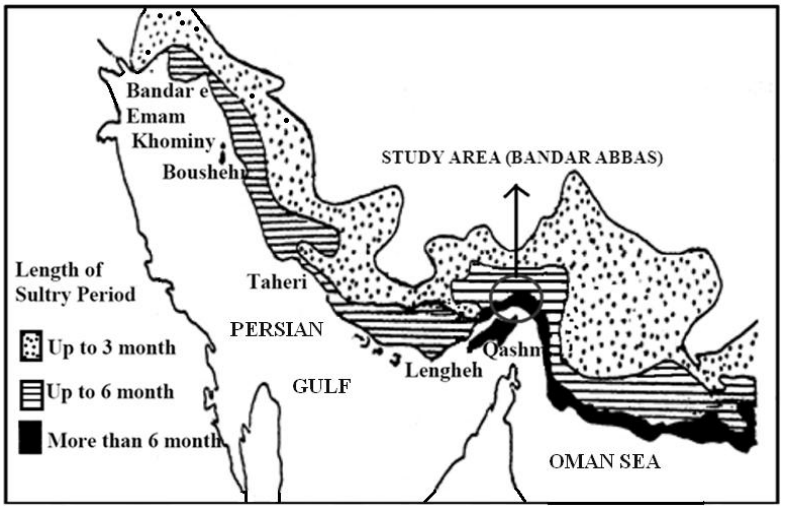


Fig.5: The sultry period in the southern coasts of the Persian Gulf (Source: Esfandiarnejad, 2010)

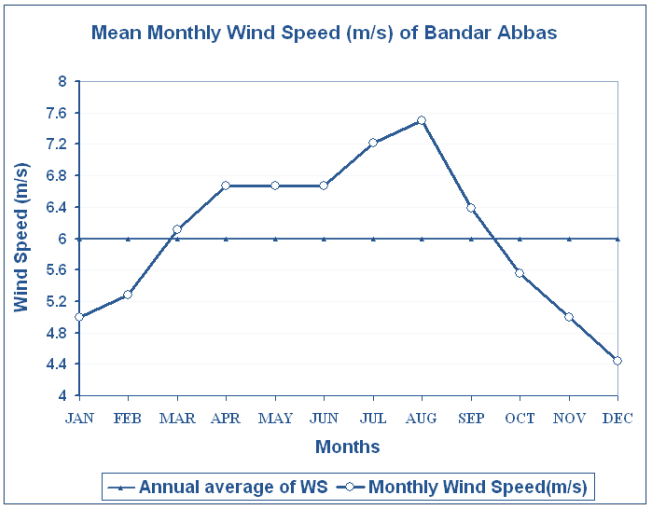


Fig.6: Monthly variation of wind speed (adapted from: IMO, 2010)

microclimatic factors could have a big role in human thermal comfort and energy performance of buildings (Najafabadi *et al*., 2006). According to Bekele *et al*. (2008), the main parameters of urban microclimate design are local climate, city location, urban density, orientation and width of the canyon, anthropogenic heat, traffic, neighbourhood shape, and distribution. The climate data of the local environment are the main parts of the microclimate analysis. The July period was selected for the evaluation of thermal comfort for the maximum thermal stress in the study area. The climate data were investigated in detail for the microclimate design considerations of the city. In addition, air movements in the selected canyons were measured in the middle of each canyon from 1st to 5th July 2010 and later compared with the data registered in the airport reference station during this time. On the other hand, the field measurements in the selected canyons indicated the strong influence of the physical features on the urban canyon microclimate.

Notably, the urban forms of Bandar Abbas are divided into three main categories: the traditional and historical fabrics, the modern and new residential developments, and the slum and sprawl fabrics. The selected canyons are located in the traditional and modern fabrics. Meanwhile, new residential developments are covered with one-story and mid-rise buildings, whereas the selected traditional fabric is covered with one-story buildings only. These forms could influence the urban microclimate differently (Thapar, 2008). The one-story buildings are formed as a dense built form, hence, resulting in a variety of environmental conditions due to the different rates of shading, temperature, air flow, and subsequently, thermal comfort condition. Fig.7 and Fig.8 show the microclimatic data charts of the study area of each canyon.

*Thermal comfort index (PET)*

The Physiological Equivalent Temperature (PET) is introduced as a model, which works based on the Munich Energy-balance Model for Individuals (Toudert & Mayer, 2007). According to Hoppe (2002), the basis of PET is the air temperature in a typical indoor setting, in which the heat share of the human body is balanced with the same core and skin temperature under the complex outdoor conditions. In addition, PET also allows the assessment of thermal conditions in a physiologically significant way. PET, as a thermal comfort index, takes into account four climatic factors that affect comfort conditions: Ta, Mean Radiant Temperature (MRT), RH%, and air movement.

Based on the goal of this study (i.e. to compare the thermal comfort conditions of different canyons and fabrics rather than calculating the exact comfort level), the Physiological Equivalent Temperature (PET) index observed in recent outdoor studies was selected for this study. Although the activity level and clothing rate are not considered in the PET index, an index with capability of considering these parameters is not necessary. Because of the significantly less variation of such parameters in the study area, the other indices, like Predicted

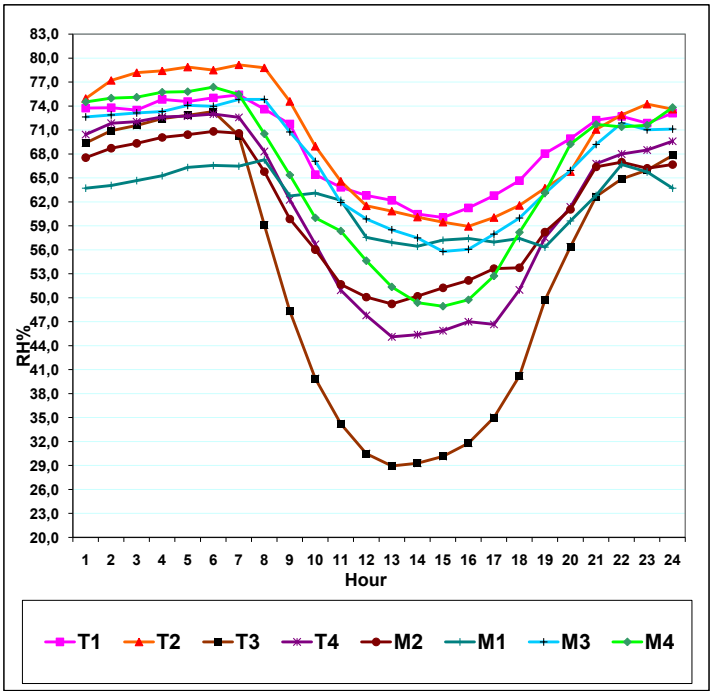


Fig.7: Variation of the recorded relative humidity in each point

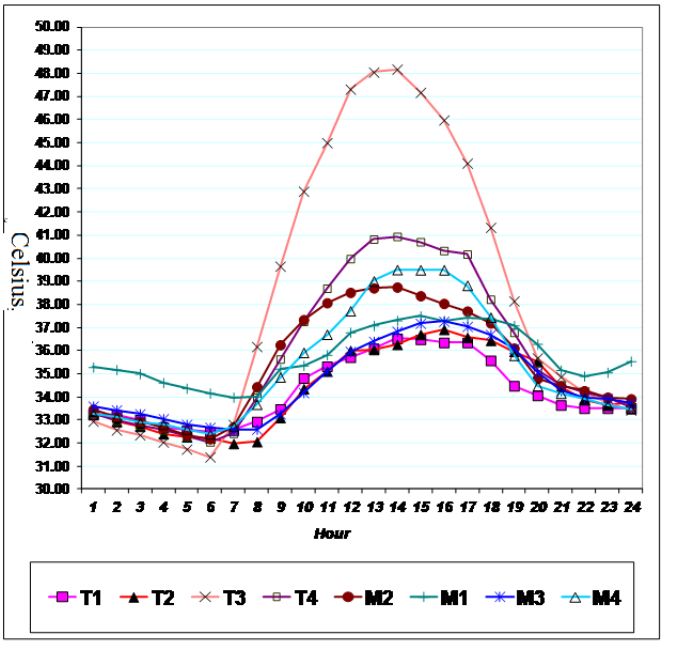


Fig.8: Variation of the recorded air temperature in each point

Mean Vote (PMV) and Standard Effective Temperature (SET), were only used for comparing the situation.

The PET index, expressed in degree Celsius, is calculated using Rayman software (Ver. 1.2). There is no suitable comfort zone for outdoor, hot and humid conditions, which defines the PET index. However, according to a study conducted in Dhaka, for hot and humid summer months, the comfort zone for a person in a shaded place with the activity level of 1 met (i.e., sedentary) and clothing rate is between 0.35 and 0.5 clo (Ahmed, 2003). The thermal comfort was found in a temperature range of 27.5 to 32.5°C, while the RH rate was between 50-75% at 32.5°C and 50-85% at 27.5%°C, only for calm conditions. In the case of existing air flow, this boundary would extend to higher comfort limits depending on wind speed, in which the increasing relative humidity could be tolerated by humans (Ahmed, 2003).

According to Ahmed (2003), if the air and radiant temperature are equal, the comfort zone corresponds to the PET limits between 27-33°C. However, this estimation is not completely acceptable. Besides, the Dhaka situation is not exactly similar to Bandar Abbas. However, the upper estimated comfort zone of PET=33°C was used as the index for the outdoor thermal comfort.

Another important factor in calculating the comfort condition is MRT. In hot humid regions, MRT is at the second degree of importance after air temperature among the environmental parameters (Emmanuel, 2005). The MRT rate for the studied urban canyons in this research, according to VDI, could be calculated as follows:

$$MRT = \left[ MRT^{*4} + \frac{f_p . a_k . I_b}{\varepsilon_p . \sigma} \right]^{0.25}$$

$$MRT^{*} = \left[ \frac{1}{\sigma} \sum_{i=1}^{n} (\varepsilon_i . \sigma . T_{s,i}^4 + \frac{a_k . I_{dj}}{\varepsilon_p}) F_i \right]^{0.25}$$

Where,

$MRT^*$ : Mean radiant temperature from long-wave and diffuse short-wave radiation (not including direct-beam radiation) (°C)

$f_p$ : Surface projection factor of a standing or walking person

$I_p$ : Beam radiation (on a plane perpendicular to the beam) ( $W/m^2$)

$a_k$ : Average (short-wave) absorptive of the human body=0.7

$\varepsilon_p$ : Emissivity of the human body=0.97 $5.67\times10^{-8}$ $W/m^2K^4$ (the Stefan-Boltzmann constant)

$\varepsilon_i$ : Emissivity of the surface

$T_{s,i}$ : Surface temperature (K)

$I_{d,i}$ : Diffuse radiation($W/m^2$)

$F_i$ : View factor of the surface

In order to estimate PET and other thermal comfort indices at the canyon level, the Hobo data loggers were installed in the eight selected canyons, and consequently, the results were shown as the average of data for a sample day of July as the hottest day of the year.

The main activities of people are leisure walking, standing and sitting by the house entrances, which corresponded to a metabolic rate of 1.2-2 met (ASHRAE, 2004). Within the study area, clothing consisted of light shirts and trousers, which corresponded to 0.4-0.5 clo. During the measurement period, the weather condition was similar and no rain or overcast condition was reported. Consequently, main factors like Ta, RH%, cloud cover and radiation condition, were reported to be stable and no major daily variation was recognized in the recorded data.

*Temperature Humidity Index (THI)*

Temperature Humidity Index (THI), which is also known as Discomfort Index (DI), is one of the variants of Effective Temperature (ET) developed by Thom (Angouridakis, 1982). This index considers and combines the wet and dry bulb temperatures as a scale to state the thermal sensation of a human being. Later, Nieuwolt modified the discomfort index as a combination of air temperature and relative humidity (as cited in Kakon *et al.*, 2010). Particularly in a case where relative humidity data are more frequently available than the wet bulb temperature, the following equation can be used:

$$THI = 0.8Ta + (RH \cdot Ta)/500$$

Where,

$$THI = 0.8Ta + (RH \cdot Ta)/500$$

Where,

Ta = the air temperature (°C)

RH = the relative humidity (%)

On the other hand, the comfort limits are defined as follows:

$21 \leq THI \leq 24$ = 100% of the subjects felt comfortable

$24 < THI \leq 26$ = 50% of the subjects felt comfortable

$THI > 26$ = 100% of the subjects felt uncomfortably hot

*Wind Flow Simulation (CFD)*

Today, the CFD models are becoming more popular as a research procedure to predict air flow and ventilation performance for outdoor and indoor spaces (Chen, 2009). Because of the changing of wind speed and direction over times and also the effects of surrounding buildings, the design of natural ventilation and air flow has become more complicated (Chen, 2009). Therefore, the CFD method was used in order to gain a proper understanding about the likely air flow within different canyons compared to the recorded field data. Basically, CFD is about numerical simulation of fluid flow processes, and it shows the air flow processes occurring inside and around building spaces (Yoshie *et al.*, 2007). The CFD method is capable to provide accurate and informative results by solving the Navier-Stokes equations as a highly reliable method (Zaho & Chen, 2011). The eight selected canyons were modelled in order to facilitate the simulating air flow in selected times and dates. The sizes and dimensions of buildings were previously mentioned in the last section. Fig.9 shows the general view of the aforementioned models.

In order to gain a great understanding of the air flow within the study areas (i.e. related buildings and canyons), the first step is to determine the physical patterns and geometry of the buildings and domain area. Moreover, to understand the impacts of terrain categories on the wind profile of the study area, two different models were considered. The ASHRAE (2004) and ASCE (the Log Law model) (1999), as a general standard (Abdul RazakBin Sapian, 2003; Tahbaz, 2007), were the main models used in this study for plotting the diagram of mean wind profile of the study area. The ASHRAE handbook (2004) equation (Tahbaz, 2007) describes the models and the fundamentals of air flow around the buildings in a table form for different environments so as to obtaining the wind speed profile (u) and height (h). The equations are as follows:

$$u(h) = u_{met}\left(\frac{\delta_{met}}{h_{met}}\right)^{\alpha_{met}}\left(\frac{h}{\delta}\right)^{\alpha}$$

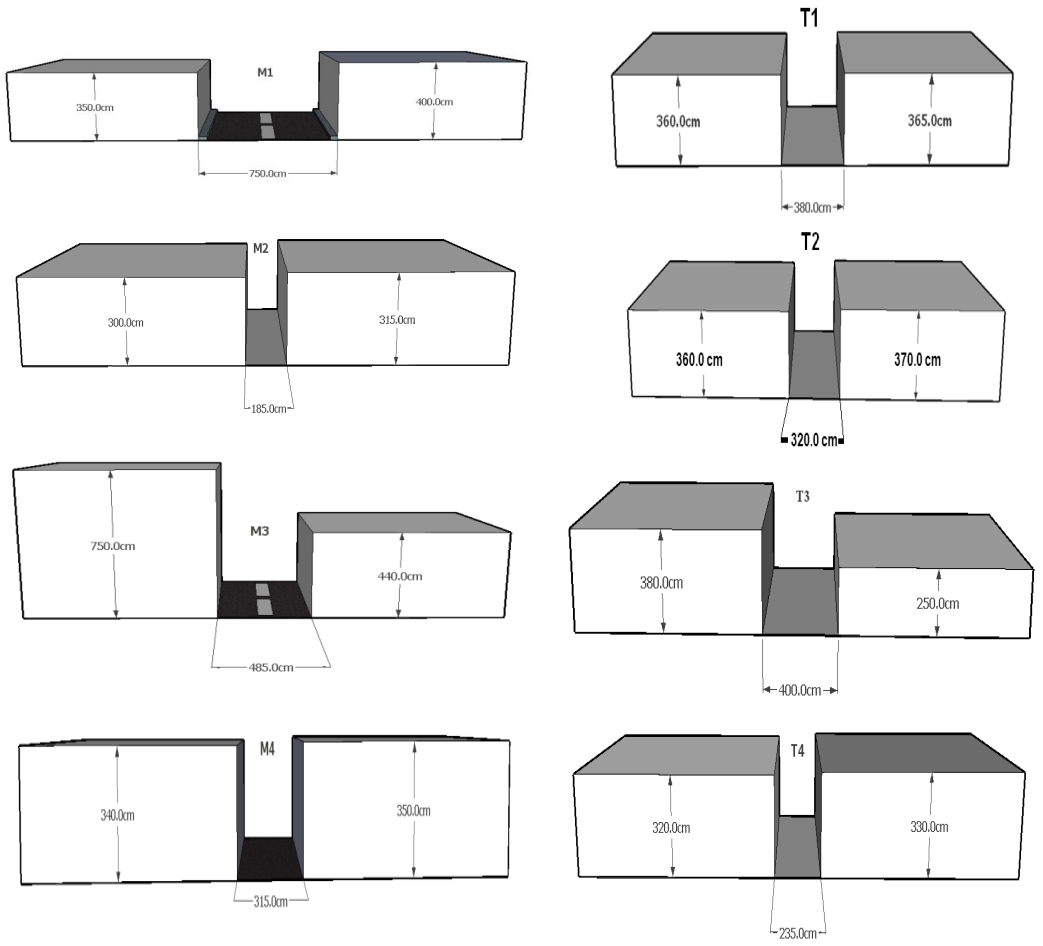


Fig.9: General view of the eight canyon models

or;

$$\frac{\overline{V}_{met10}}{\overline{V}_{z10}} = \frac{\left[\frac{met_{10}}{met_G}\right]^{\alpha_{met}}}{\left[\frac{Z_{10}}{Z_G}\right]^{\alpha}}$$

Where,

δ met = 270 m is the *layer thickness* for the meteorological site (assumed to be of the 'Country' type)

$\alpha$ met = 0.14 is the *exponent* for the meteorological site (assumed to be of the 'Country' type)

*h* met = is the *measurement height* for the meteorological site (assumed to be 10 m)

Meanwhile, the ASCE (1999) equation (Sapian, 2009) is as follows:

the Log Law model:

$$V_Z = V_{ref}[\log(Z / Z_0) / \log(Z_{ref} / Z_0)]$$

Where,

Vz = mean wind speed at height Z
Vref = mean wind speed at some
Zref = reference height
Z = height for which the wind speed Vz is computed
Zo = roughness length or log layer constant

To explain the mean wind speed profile above the canyon level at height Z, these two equations are the auxiliary method for justifying and controlling the simulations of wind speed profile inside the canyon level according to the field measurements.

According to the average data of wind speed (1959-2005), the mean wind speed in July was 6m/s. The wind profile of the study area had been plotted using the Log Law model (Sapian, 2003) and the ASHRAE adopted model (ASHRAE, 2004; Tahbaz, 2007), while the reference station wind speed of 6m/s was considered. The plotted data showed the numerical variation of wind speed inside the canyons level.

In order to conduct the CFD simulation for the selected canyons, the following steps using the MicroFlo (IESve) software application were carried out for each canyon in terms of date, time, wind speed (m/s), and wind direction. Based on the size of each model, a 3D boundary (computational domain) was assigned, depending upon the CFD setting (Wesseling, 2001). Notably, the simulated air flow depended on the physical factors, such as the building layout, canyon dimension and orientation, as well as upwind specification and microclimate situation of the study area. The next step is to run the simulation, and the software displays the velocity results on the Z-grid in axonometric view. This allows the users to see the contouring throughout the model (IES, 2009). However, the results of the external CFD simulation in MicroFlo was contour base displaying.

## DATA ANALYSIS AND RESULTS

The conducted analyses and the results of the collected data are presented visually as graphs, tables, and charts. Establishing

the rational relationships between the field measurements, CFD simulations, and thermal comfort investigations, as well as the interpretation of results is the main aim of this section. According to the calculated comfort indices and microclimate data of the study area, each canyon had different environmental characteristics and thus varying comfort situations. The main aim of urban design in hot-humid regions is to provide thermal comfort. Therefore, open spaces which allow breeze to pass through have a better condition of comfort as compared to semi-enclosed and enclosed spaces which are not along the prevailing wind. Besides, restricted free air flow is in the discomfort condition during the summer period. The adapted microclimate and thermal comfort investigation with the CFD simulation method serve to articulate the subjective nature of the collected field data and to examine the linkages among the referred methods.

This section is divided into two sub-sections so as to reflect on the following subjects in the selected canyons separately, namely, the specifications of thermal comfort situation, and the air movement simulation and prediction.

*Specifications of the Thermal Comfort Situation*

The calculated thermal comfort indices (Fig.10 and Fig.11) were estimated for the sample's hottest day of the year on July 1st, 2010 to indicate the upper limits of the comfort zone, with the air flow of 1 m/s and the average data of Ta and RH% obtained during the study period from 1st to 10th July 2010. Meanwhile, the highest rate of each index in the canyons of the traditional fabric at the peak of the day's temperature was around 3°C lower than those of the modern fabric. In general, the canyons with the N-S and SSE-NNW orientations showed lower rates of the calculated indices due to the

TABLE 5
Variation of thermal comfort indices during the days in July (min. and max. values)

| Canyon | Ts/°C | | Ta/°C | | Tmrt/°C | | PMV | | PET/°C | | SET*/°C | |
|---|---|---|---|---|---|---|---|---|---|---|---|---|
| | Min. | Max. | Min. | Max. | Min. | Max. | Min. | Max. | Min. | Max. | Min. | Max. |
| T1 | 29.7 | 50.6 | 33.5 | 36.5 | 24 | 66.1 | 2 | 5.1 | 28.8 | 49.1 | 24.7 | 38.7 |
| T2 | 29.9 | 47.1 | 32.2 | 36.3 | 24.3 | 64.5 | 2.1 | 4.8 | 29 | 47.1 | 24.9 | 37.3 |
| T3 | 29.6 | 68.9 | 31.4 | 48.2 | 23.9 | 77.2 | 1.9 | 8.1 | 28.8 | 65.3 | 24.5 | 49.6 |
| T4 | 29.7 | 57.4 | 32 | 4.9 | 24.1 | 70.4 | 2 | 6.3 | 28.9 | 55.7 | 24.7 | 43 |
| M1 | 30 | 60.3 | 32.2 | 38.8 | 24.4 | 69.6 | 2 | 6 | 29.2 | 54.4 | 24.9 | 43 |
| M2 | 31.6 | 58 | 34.2 | 37.3 | 26 | 69.1 | 2.3 | 5.9 | 30.5 | 53.6 | 26 | 42.2 |
| M3 | 29.9 | 61 | 32.7 | 36.8 | 24.2 | 67.6 | 2 | 5.7 | 29 | 52.5 | 24.8 | 41.9 |
| M4 | 29.7 | 55.9 | 32.4 | 39.5 | 24.1 | 67.9 | 2 | 5.7 | 29.2 | 52.4 | 24.7 | 40.5 |

significantly higher rates of air flow. Table 5 presents the maximum and minimum rates of the calculated thermal comfort indices for each canyon.

As shown in Fig.12, the discomfort index of the eight selected sites, in which the data were collected during the hottest period of a year, indicated a discomfort condition during the whole hours of the day. However, it should be mentioned that the effects of air flow and shadows were not considered in this index. The calculated discomfort index for January, as compared to July, indicated different thermal comfort situations in the moderate and hottest months.

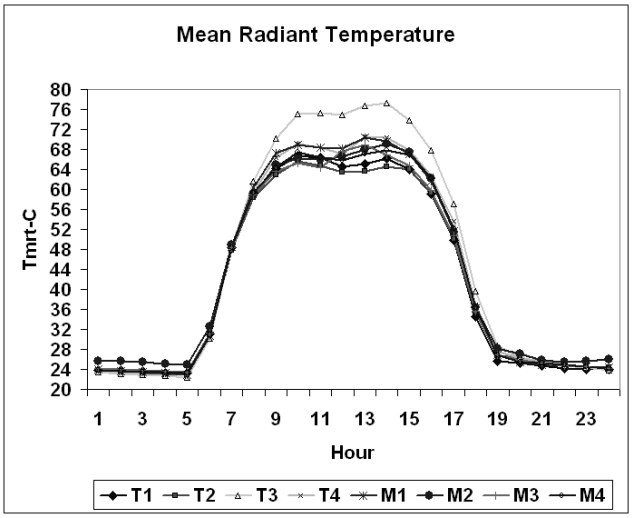


Fig.10: Mean radiant temperature (Tmrt) inside the canyons

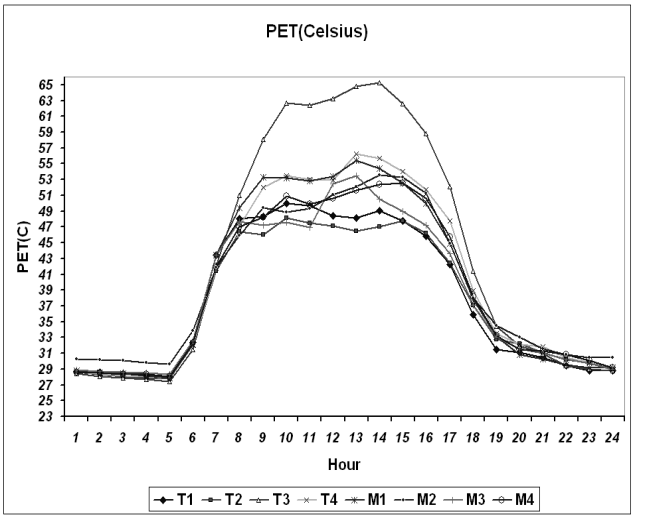


Fig.11: PET (°C) inside the canyons

*Air Movement Simulation and Prediction*

The mean wind speed profile, which had been plotted for the study area according to the ASHRAE and ASCE models (ASHRAE, 2004) shown in Fig.13, illustrates the vertical profile of wind speed in the canyons level from 0 to 10m heights (Tahbaz, 2007). Fig.13 presents a comparison of two different wind profile modellings conducted according to the study area conditions. The plotted wind profile in the study area showed a dissimilar variation of height to speed ratio, especially between 2 to 6 meter levels. According to the registered data of field measurements (which was in 2 meter height) shown in Table 6, the ASCE (1999) model was more reliable than ASHRAE.

Fig.14 reveals the wind simulation results of the selected canyons for each one of the study sites in both the traditional and modern fabrics, separately. The simulated and recorded wind speeds had a reasonable relation in terms of calculated mean speed and calculated correlation coefficient (Table 6). The selected data of the recorded and simulated wind speeds explained the swing rate hours of wind magnitude in a day. The wind speed rate changed to stronger from 8 am and reached the peak around 2 to 3 pm, and then went to zero m/s around 8 to 00 pm (see Fig.15).

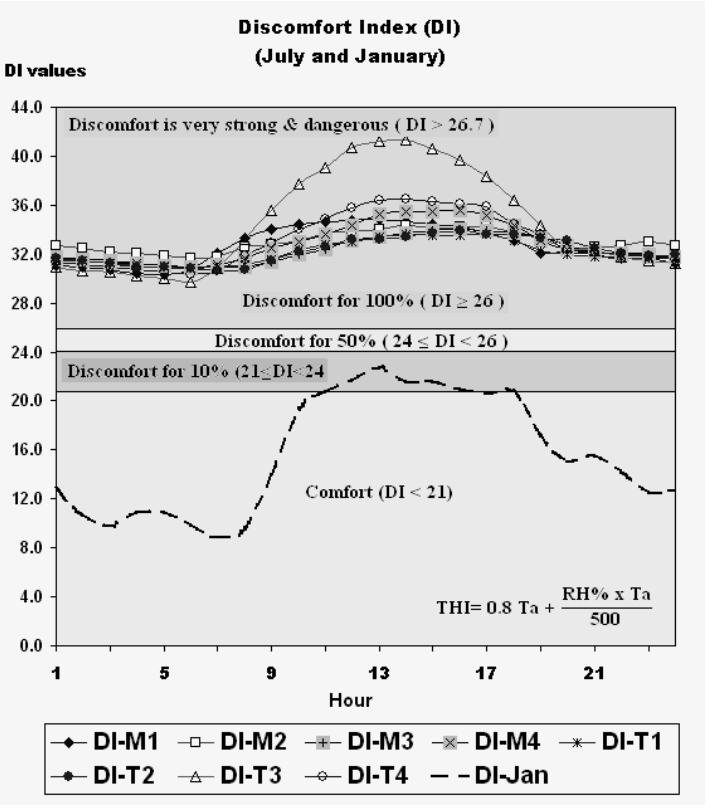


Fig.12: Discomfort index (DI) in January (entire area) and July for the eight selected canyons

According to the CFD results, the selected canyons showed different characteristics in the recorded wind speeds but the simulated wind speeds were more similar to the recorded ones in all the canyons. Fig.14 and Fig.15 indicate the differences in wind speeds recorded during the study period, in which higher air movements were reported for the traditional fabrics, especially between 12 pm to 15 pm.

The main difference between the canyons with the N-S and WSW-ENE orientations in this research could be the recorded wind speeds. Based on the measured data of wind speed in the selected canyons and the reference station, one may observe that the recorded wind speed data could be divided into three main daily periods. The first period was between 00 to 8 am, with a calm period around 0-0.1 m/s speed. The second period was between 8 am to 8 pm, which stated the wind speed had gradually increased to the highest speed at around 2 or 3 pm and went down around 8 pm in concordance with the results found on the field and simulations. Finally, the third

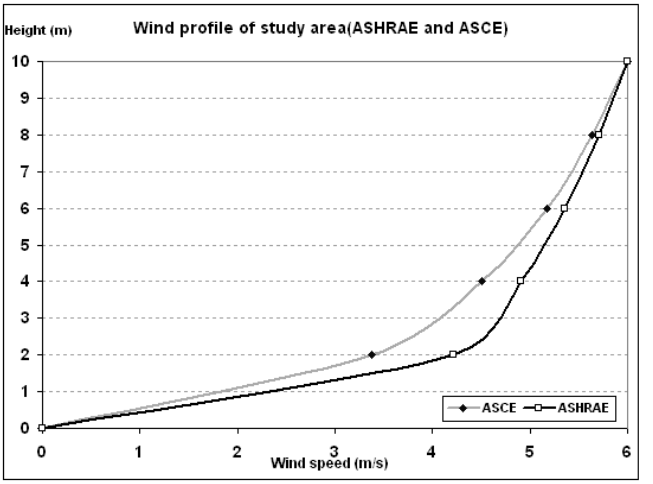


Fig.13: Mean wind profile using the ASHRAE and Log Law (ASCE, 1999) models

TABLE 6
Recorded and simulated wind speed (m/s) data with correlation coefficients (cc) for each canyon

| Hour | T1 | | T2 | | T3 | | T4 | | M1 | | M2 | | M3 | | M4 | |
|---|---|---|---|---|---|---|---|---|---|---|---|---|---|---|---|---|
| | Rec. | Sim. | Rec. | Sim. | Rec. | Sim. | Rec. | Sim. | Rec. | Sim. | Rec. | Sim. | Rec. | Sim. | Rec. | Sim. |
| 8 am | 0.06 | 0.06 | 0.2 | 0.27 | 0.1 | 0.31 | 0.1 | 0.3 | 0 | 0.06 | 0.47 | 0.56 | 0 | 0.24 | 0.1 | 0.25 |
| 12 pm | 1.8 | 1.71 | 2.8 | 1.95 | 0.65 | 0.71 | 1.5 | 1.39 | 0.75 | 0.89 | 1 | 0.89 | 1.4 | 1.7 | 1.1 | 1.29 |
| 2 pm | 2 | 1.56 | 2.85 | 2.02 | 0.8 | 0.6 | 1.2 | 1.16 | 0.3 | 0.4 | 0.9 | 0.73 | 1.5 | 1.74 | 2.2 | 2.11 |
| 8 pm | 0.8 | 0.68 | 0.86 | 0.91 | 0.17 | 0.19 | 0.3 | 0.43 | 0.7 | 0.55 | 0.9 | 0.88 | 0.6 | 0.66 | 1.4 | 1.04 |
| Mean Speed (m/s) | 1.2 | 1.0 | 1.7 | 1.3 | 0.4 | 0.5 | 0.8 | 0.8 | 0.4 | 0.5 | 0.8 | 0.8 | 0.9 | 1.1 | 1.2 | 1.2 |
| CC | 0.99 | | 0.99 | | 0.89 | | 0.99 | | 0.93 | | 0.92 | | 0.99 | | 0.96 | |

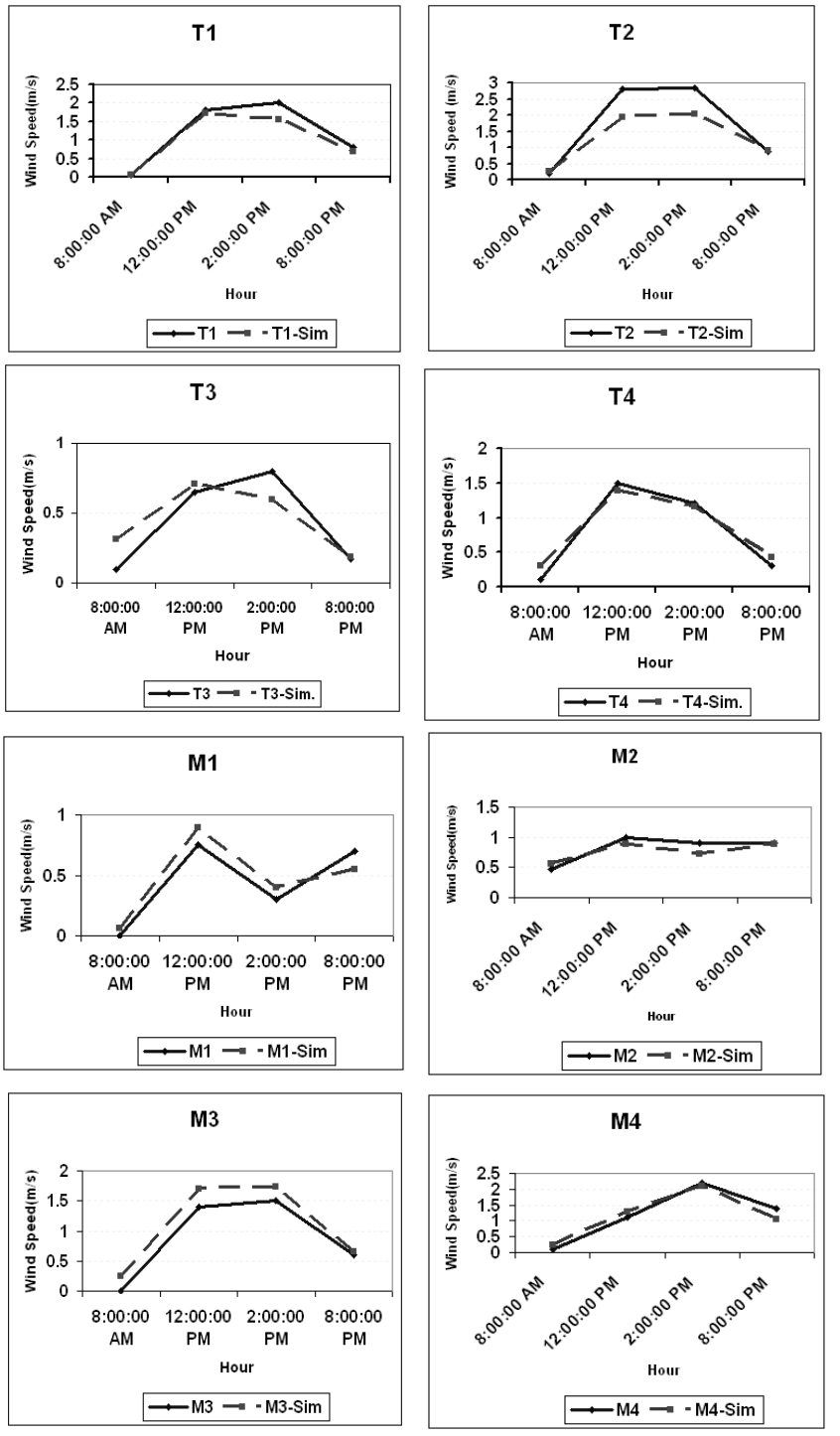


Fig.14: Comparison graphs of the recorded and simulated wind speeds inside the canyons

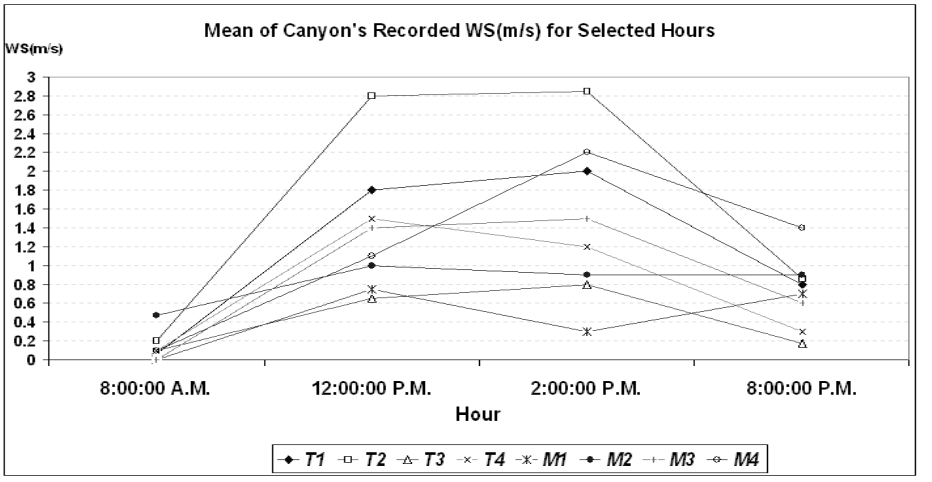


Figure 15: Wind speed range (mean values) during selected hours for each canyon

period was between 8 pm to 12 midnight, in which the wind speed reduced to 0 m/s. This finding shows that the wind speed trend went according to the temperature range, and consequently, the sea and land breezes connected to the air pressure variations. The highest peak of the daily temperature and wind speed occurred at the same time and vice versa. The daily variation of wind speed in July at the meteorological station and the selected canyons seemed to be very representative of the general conditions found in the whole urban area.

## CONCLUSION

This study concludes that, in July, which is the hottest month of a year, the outdoor thermal comfort of the study area (i.e., Bandar Abbas, Iran) was higher than the maximum comfort zone for all canyons. In general, the results indicated lower thermal comfort values (i.e. PET, PMV, SET and Tmrt) in the traditional fabric canyons with the N-S orientation compatible with the prevailing southward winds by more than 3°C. Higher wind speeds were registered in the N-S oriented canyons compared to the other canyons with different orientations. The daily variation of wind speed showed the maximum speed between 12 pm to 16 pm, whereas in the canyons with the N-S orientation, the wind reached as high as 3.75m/s, which consequently improved the comfort zone by reducing the humidity level.

Computational Fluid Dynamic (CFD) and particularly the MicroFlo (IESve) software were found to be accurate tools to simulate and predict the air flow (wind speed) in the urban canyons of Bandar Abbas, Iran. The correlation coefficients of the measured and simulated wind speeds in all cases, except for T3, were more than 92%, which means that, CFD has a good potential to address the condition of air flow in the study area.

The above results revealed that the CFD procedures conducted in this research are valid and therefore could be applied to similar studies. Therefore, the methods used in this study are reliable alternative for future assessments of wind flow in urban residential canyons and outdoor spaces to obtain accurate experimental data.

## REFERENCES


ASHRAE. (2004). Thermal environmental conditions for human occupancy. In A. society of & refrigerating and air-conditioning Engineers heating (Eds.) *ASHRAE Standard 55*, *Atlanta* (pp. 34-39). New York: SAGE.

Ahmed, K. S. (2003). Comfort in urban spaces: defining the boundaries of outdoor thermal comfort for the tropical urban environments. *Energy and Buildings, 35*(1), 103-110.

Alaedini, P., Zebadast, E., & Mousavi, K. (2008). *Land market and housing dynamics in low income settlement in Iran: Examining data from three cities*. World Bank and Government of Iran. (UUHRP), pp. 17-19.

Angouridakis, V. E., & Makrogiannis, T.J. (1982). The discomfort index in Thessaloniki, Greece. *International J of Biometeorology, 26*(1), 53-59.

Azari NajafAbadi, K., Pakseresht, S., & Pooryousefzadeh, S. (2006). *Role of Wind in Vernacular Architecture of Hot and Humid Region of Iran*. Symposium on Improving Building Systems in Hot and Humid Climates.

Balázs, B., Hall, T., Roth, M., & Norford, K. (2009). *Microclimate in a high-rise residential development in Singapore. Urban Climate*. The seventh International Conference on Urban Climate (p 245-278). Japan: Yokohama.

Bekele, S., Johns, I., & Gokul, I. (2008). Microclimate Study of a City in Hot and Humid Climate. New York: SAGE Publication.

Chen, Q. (2009). Ventilation performance prediction for buildings: A method overview and recent applications. *Building and Environment, 44*(4), 848-858.

Chen, Q, Pan, N., & Guo, Z. Y. (2011). A new approach to analysis and optimization of evaporative cooling system II: Applications. *Energy, 36*(5), 2890-2898.

Creswell, J. W. (1994). *Research design (Qualitative & Quantitative Approaches)*. London: Saga Publications.

Emmanuel, R. (2005). Thermal comfort implications of urbanization in a warm-humid city: the Colombo Metropolitan Region (CMR), Sri Lanka. *Building and Environment, 40*(12), 1591-1601.

Esri. (2008). *ArcGIS Software Version 9.x*. Redlands, California: Esri Corporation, www.Esri.com.

Ghobadian, V. (1998). *Climatic Survey of Traditional buildings of Iran*. Tehran-Iran: Tehran University Press.

Givoni, B. (1998). *Climate Consideration in Building and Urban Design* (p. 464). London: John Wiley & Sons.

Hamdan, M., Kandar, M., & Roshia, A. (2007). *Comfortable housing model in new housing PPRT for Orang Asli*, Universiti Teknologi Malaysia. UTM.

Heidari, S., & Sharples, S. (2002). A comparative analysis of short-term and long-term thermal comfort surveys in Iran. *Energy and Buildings, 34*(6), 607-614.

Hoppe, P. (2002). Different aspects of assessing indoor and outdoor thermal comfort. *Energy and Buildings, 34*(6), 661-665.

IES. (2009). *Microflo (CFD) user guide.* Integrated Environmental Solutions Limited (IES).

IMO. (2010). *46 years Weather Data of Bandar Abbas (1959-2005)*. Meteorological Organization of Iran. Tehran: ISD publications.

Johansson, E. (2006). Influence of urban geometry on outdoor thermal comfort in a hot dry climate: A study in Fez, Morocco. *Building and Environment, 41*(10), 1326-1338.

Kakon, A. N., Nobou, M., & Yoko, S. (2010). Assessment of thermal comfort in respect to building height in a high-density city in the tropics. *American J. of Engineering and Applied Sciences, 3*(3), 545-551.

Krüger, E. L., Minella, F. O., & Rasia, F. (2010). Impact of urban geometry on outdoor thermal comfort and air quality from field measurements in Curitiba, Brazil. *Building and Environment, 46*(3), 621-634.

Muller, A. (2005). *User Manual of Counter Anemometer Model: 91g*. Germany-Chausseestraße: Meteorologische Instrumented K G R. FUESS.

Nunez, M., & Oke, T. R. (1977). The Energy Balance of an Urban Canyon. *Journal of Applied Meteorology, 16*(1), 11-19.

Onset. (2004). *Hobo Micro Station User's Guide*. USA: Onset Computer Corporation.

Sapian, A. R. (2003). *Possibilities of using void to improve natural cross ventilation in high-rise low cost residential building*. Faculty of Built Environment. Universiti Teknologi Malaysia.

Sharmand. (2008). Revision of Bandar Abbas Master Plan. In Sharmand Consulting Engineers (Ed.), *Housing and Urbanization Organization of Hormozgan Province* (pp. 12-19). Tehran, ISC Publication.

Shohouhian, M., & Soflaee, F. (2005). *Environmental sustainable Iranian traditional architecture in hot-humid regions*. International sustainable Passive and Low Energy Cooling for the built Environment. Santorini, Greece.

Sullivan, J., & Collins, J. (2009). The use of low-cost data logging temperature sensors in the evaluation of an urban heat island in Tampa, Florida. *Applied Geography Conference* (pp. 10-25). Fort Worth, Texas.

Tahbaz, M. (2007). *The Estimation of the Wind Speed in Urban Areas*. Tehran: School of Architecture and Urban Planning Shahid Beheshti University Press.

Thapar, Y.H. (2008). *Microclimate and Urban Form in Dubai*. PLEA-25th Conference on Passive and Low Energy Architecture (pp. 123-143). Ireland: Dublin.

Toudert and Mayer. (2007). Effects of asymmetry, galleries, overhanging facades and vegetation on thermal comfort in urban street canyons. *Solar Energy, 81*(6), 742-754.

Wei, J., Zhao, J., & Chen, Q. (n.d.). Energy performance of a dual airflow window under different climates. *Energy and Buildings, 42*(1), 111-122.

Wesseling, P. (2001). *Principles of Computational Fluid Dynamics*. New York: Springer.

Yoshie, R., Mochida, A., Tominaga, Y., Kataoka, H., & Harimato, K. (2007). Cooperative project for CFD prediction of pedestrian wind environment in the Architectural Institute of Japan. *Wind Engineering and Industrial Aerodynamics* (95), 1551-1578.

Yu, C., & Hien, W.N. (2006). Thermal benefits of city parks. *Energy and Buildings, 38*(2), 105-120.